colloids and interfaces

MDPI

Article

Conductive Nanofilms with Oppositely Charged Reduced Graphene Oxides as a Base for Electroactive Coatings and Sensors

Tomasz Kruk * and Piotr Warszyński *

Jerzy Haber Institute of Catalysis and Surface Chemistry, Polish Academy of Sciences, Niezapominajek 8, 30-239 Kraków, Poland

* Correspondence: tomasz.kruk@ikifp.edu.pl (T.K.); piotr.warszynski@ikifp.edu.pl (P.W.)

Abstract: We demonstrate a method for the formation of multilayers composed of reduced graphene oxide (rGO), which can be used for transparent, conducting thin films. Using the layer-by-layer (LbL) assembly of positively and negatively charged GO sheets, we could obtain thin films with highly controllable sheet resistance. The natural negative charge of graphene oxide was turned to positive by the amidation reaction. After forming the multilayer films, the graphene oxide underwent thermal reduction at temperatures above 150 °C. The (rGO^+/rGO^-) films were characterized by UV-Vis and scanning electron microscopy (SEM), and their conductivity was measured by the four-point method. We found that after deposition of five (rGO^+/rGO^-), the coating structure reached the percolation limit, and the film resistance decreased more gradually to around 20 kΩ/sq for the films obtained by eleven deposition cycles with graphene oxide reduced at 250 °C. The formation of thin films on polyimide allows the forming of new flexible conductive materials, which can find applications, e.g., in biomedicine as new electroactive, low-cost, disposable sensors.

Keywords: graphene oxide; multilayer films; layer-by-layer; conductive coatings; electroactive sensors

Citation: Kruk, T.; Warszyński, P. Conductive Nanofilms with Oppositely Charged Reduced Graphene Oxides as a Base for Electroactive Coatings and Sensors. *Colloids Interfaces* **2021**, *5*, 20. https://doi.org/10.3390/colloids5020020

Academic Editors: Alexander Kamyshny and Victor Starov

Received: 31 January 2021
Accepted: 29 March 2021
Published: 1 April 2021

1. Introduction

Graphene, a two-dimensional carbonaceous nanomaterial, has been recently an object of intensive research regarding its electrical, chemical and mechanical properties [1–5]. However, it is poorly dispersed in polar and apolar solvents, which limits many potential applications [4]. In particular, in water, it has a tendency to agglomerate into graphite. Therefore, the modification of graphene sheets appears necessary for its applications in nanoelectronic-, chemistry-, and physics-based technologies or bio-medical devices. Moreover, high-quality graphene formation at a low cost is still a technological challenge [6].

Graphene oxide (GO) is one of the covalently modified graphene forms that can be easily manufactured by chemical exfoliation [5]. GO is formed of single atomic layers of graphene-like structures with a mixture of carbon atoms with sp^2 and sp^3 hybridization and a high density of epoxy and hydroxyl groups on both sides of the basal carbon planes and carboxyl groups around their edges [7]. GO sheets are hydrophilic and can form stable dispersion in an aqueous medium [8,9]. Graphene oxide can be partially reduced to reduced graphene oxide (rGO) using various chemical, electrochemical, thermal, hydrothermal, and photothermal reducing techniques [10,11]. During the reduction, the oxygen-containing groups are partially eliminated from the graphene oxide surfaces and the sp^2 hybridization of carbon's electronic orbitals is reformed [12–14]. The electrical conductivity of the graphene structure is partly regained, and rGO can be dispersed in various solvents [15], including water, forming stable suspensions that can be used for deposition on various surfaces. Additionally, due to the presence of hydrophobic (basal planes) and hydrophilic domains, rGO is amphiphilic and can be used for foam or Pickering emulsions stabilization [16,17]. Furthermore, the functional groups remaining after the reduction process facilitate covalent modification by attachment of various functional groups, ligands, etc. [18,19].

Various approaches have been investigated to assemble GO or chemically modified graphene sheets into films with tailorable properties and architectures, including direct chemical vapor deposition (CVD) [20,21], vacuum filtration [22,23], spin-coating [24], and Langmuir–Blodgett assembly [25,26]. However, the sequential adsorption method, also referred to as the layer-by-layer (LbL) technique [27], is one of the simplest and most promising techniques to form graphene-based nanocomposite coatings [28–33].

The graphene-based LbL method was first showed by Kotov in 1996 [34] using non-exfoliated graphite oxide platelets and polyelectrolytes. Pristine graphene oxide is negatively charged; it can be suspended in water and used as an anionic layer for the film build-up. A well-exfoliated graphite oxide sheet was used with cationic polyelectrolyte for LbL growth by Kovtyukhova et al. [35]. Yang et al. demonstrated that the LbL-assembled PEI/GO films on a PET showed a low oxygen permeability with improved H_2/CO_2 selectivity and high transparency [36]. Gas barrier properties of multilayer membranes were investigated as a function of the GO suspensions' pH [37,38]. Gross et al. constructed the multilayers films with GO and cationic polymer poly(diallyldimethyl ammonium chloride) for gas and liquid phases chemical sensing [39]. Pajor-Świerzy et al. combined rGO and Prussian Blue nanoparticles to produce electrocatalytically active multilayer films [32]. Recently, Dos Santos et al. used negatively and positively charge rGO to form multilayer films as solution-gated field-effect transistors [40]. Yang et al. [31] and Lee et al. [41] published a comprehensive review of the applications of the LbL constructed graphene films as transparent conducting films, field-effect transistors, supercapacitors, or sensors. Prospective applications of the LbL formed films with rGO due to their high electrical conductivity are neuronal interfaces [42] or immunosensors [43]. All these reports show that the LbL assembly of graphene derivatives offers a unique opportunity to design various nanocomposites with desired properties and new material applications.

The sheet resistance of the rGO films deposited by the LbL technique and annealed at 1000 °C in an H_2 atmosphere was studied by Lee et al. [30]. Zhu and He used hydrazine and poly(diallyldimethylammonium) chloride to reduce GO and turn it to positively charged. Then they constructed rGO films with up to 30 deposition cycles on glass and poly(ethylene terephthalate) with the sheet resistance above 500 kΩ/sq [44]. In our previous paper, we proposed a simple strategy for creating multilayer thin films of reduced graphene oxide (rGO) with polycation polyethyleneimine (PEI) via layer-by-layer assembly [33]. The method was based on the formation of multilayer films with graphene oxide followed by thermal reduction of the entire film structure at temperatures below 300 °C. We obtained films with a sheet resistance of ~20 kΩ/sq in the case of those formed on quartz plates and ~40 kΩ/sq for those formed on polyimide foil. Those conductivity values were comparable to the results reported previously [45–49]. In this work, we extended those studies and used the positively (GO^+) and negatively charged (GO^-) suspensions of graphene oxide and polyelectrolytes to form multilayer films. The positively charged graphene oxide was formed by the amidation reaction. After forming $(GO^+/GO^-)_n$ films, they underwent thermal reduction at temperatures above 150 °C. Next, the $(rGO^+/rGO^-)_n$ films were characterized by UV-Vis and scanning electron microscopy (SEM), and their resistance was measured by the four-point method. We showed that high reduction temperatures (above 250 °C) and a large number of (rGO^+/rGO^-) deposition cycles are not needed to obtain comparable values of surface sheet resistance with ones reported in the literature. The use of lower temperatures for GO reduction allows using more thermally sensitive substrates and sustaining functional groups at the rGO surface that may be utilized for further functionalization. We compared the conductivity of those purely rGO multilayers with the composite ones built with rGO^- and the polycation (PEI), or rGO^+ with the polyanion-polystyrene sulphonate (PSS) deposited and reduced at the same conditions, which can be considered the main novelty of our work. The conductive films with reduced graphene oxide can be an alternative due to the high costs of graphene synthesis and adsorption.

2. Materials and Methods

Graphene oxide was obtained from Abalonyx AS (Oslo, Norway). Poly(sodium 4-styrenesulfonate) (PSS, MW ~70 kDa), ethylenediamine (99% purity), *N*-(3-Dimethylamino propyl)-*N*′-ethylcarbodiimide hydrochloride (purum ≥98%, (AT), EDC), and cellulose dialysis bags (MWCO 12,400 Da, high retention 99.99%, width 32 mm) were acquired from Sigma-Aldrich (Poznań, Poland). NaCl (99.5%), 96% H_2SO_4 analytical grade, 30% hydrogen peroxide, and 99% 2-propanol (isopropanol) analytical grade were purchased from Avantor Performance Materials Poland S.A. (Gliwice, Poland). The silicon wafers with the orientation <100> (±0.5°) were purchased from On Semiconductor (Rosnov, Czech Republic) and quartz plates from Continental Trade (Warsaw, Poland). Polyimide foil was obtained from IZO-ERG SA (Gliwice, Poland). The distilled water was taken from the Millipore Direct-Q 5UV purification system (18 MΩ cm^{-1}). All experiments were carried out at 22 °C.

2.1. Graphene Oxide Characterization

The hydrodynamic diameter measurement of graphene oxide was carried out by Dynamic Light Scattering (DLS). The zeta potential measurements were conducted using LDE (Laser Doppler Electrophoresis). The experiments were performed using the Zetasizer Nano Series (Malvern Instruments, Malvern, United Kingdom). The concentration of graphene oxide of the suspension was 0.5 g/L in 0.015M NaCl. The determination of stability for graphene oxide suspensions was based on analyzing the time-dependent changes of their size distribution and adsorption measurements.

2.2. Graphene Oxide Modification Procedure

The aim of the modification of graphene oxide was to change its charge from negative to positive and then use the positively charged GO to form multilayer films with high surface conductivity. The selected method of graphene oxide amidation was described by Hwang et al. [50]. To obtain GO^+, 1.25 g EDC (purum ≥ 98%) and 10 mL of ethylenediamine (99% purity) were mixed with 100 mL of the negatively charged graphene oxide suspension (concentration 0.5 mg/mL). The mixture was left for 12 h and stirred with a magnetic stirrer. The obtained suspension was dialyzed in MWCO 12,400 Da dialysis bags for four days to remove unreacted products (EDC and ethylenediamine). The obtained brown GO^+ aqueous dispersion was stable. Before using the GO^+ suspension for multilayer film formation, its pH was adjusted to 3.5.

2.3. Formation of Polyelectrolyte Films with Reduced Graphene Oxide Nanosheets

Silicon wafers, quartz plates and polyimide foil were used as substrates for multilayer films deposition. The selection of materials for conductive film deposition and characterization was based on the low conductance of the support. Before film adsorption, silicon wafers and quartz plates were cleaned in the piranha solution (96% H_2SO_4 and 30% H_2O_2 in 2:1 ratio). Then they were rinsed with distilled water ten times and boiled in distilled water at 80 °C for 30 min. This pretreatment caused the creation of a uniform silicon oxide layer on the top of the silicon wafers. The polyimide foil was cleaned using isopropanol and distilled water.

The solution of polyelectrolyte and suspension of GO^- and GO^+ were prepared using distilled water. The pH was measured with a pH electrode (Multifunction Meter CX-505 Elmetron, Elmetron, Zabrze, Poland) and was 6.4 for graphene oxide and 3.5 for modified graphene oxide. The $(GO^+/GO^-)_n$ films were formed using the LbL technique by n GO^+/GO^- deposition cycles from the suspensions of 0.5 g/L concentration and the ionic strength of 0.015 M NaCl. In the first step, the substrate was immersed in the suspension of positively charged graphene oxide GO^+ for 20 min and rinsed in pure water (the aim of rinsing was to remove loosely adsorbed GO^+ from the substrate). Then, the substrate within the GO^+ layer was immersed in negatively charged graphene oxide suspension (GO^-) for 20 min and rinsed, which led to the completion of a single GO^+/GO^- deposition

cycle at the substrate. That procedure was repeated to obtain the film with a required number of cycles. The same procedure was applied for the formation of $(GO^+/PSS)_n$ films. The adsorption of polyanion was performed from the 0.5 g/L PSS solution, with a pH of 5.7 and 0.15 M NaCl ionic strength.

After the multilayer film formation, graphene oxide was reduced by the thermal method at different temperatures: 150 °C, 180 °C, and 250 °C for 12 h in an ambient atmosphere. The details of the procedure of the reduction of GO to rGO were described previously [33], where its efficiency was evidenced by monitoring changes in the FTIR and XPS spectra. The schematics of the amidation of graphene oxide and the deposition of the LbL films with graphene oxide are shown in Figure 1.

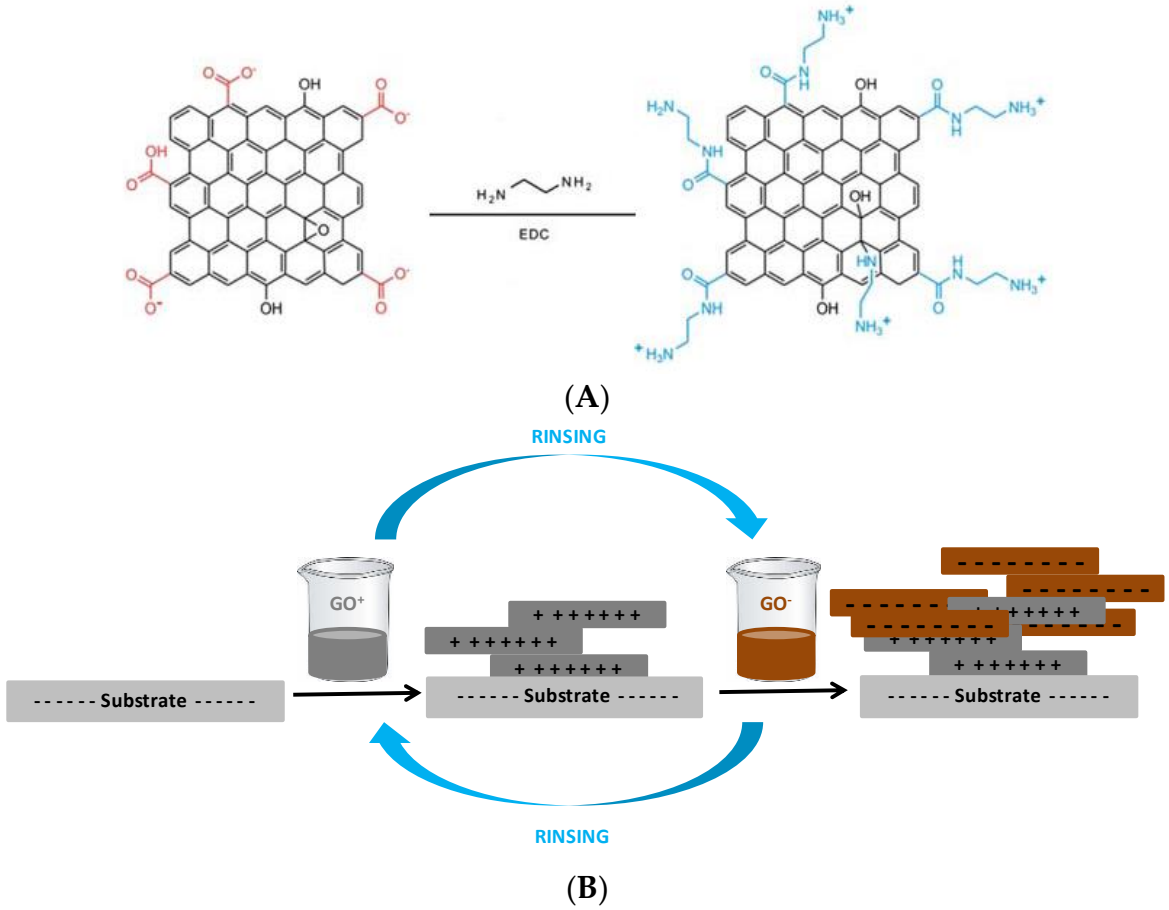

Figure 1. (**A**) Schematics of the chemical modification of GO (redrawn from [50]); (**B**) representation of the LbL assembly of the GO multilayer with GO-COO^- and GO-NH_3^+ followed by thermal reduction.

2.4. Characterization of Polyelectrolyte Films with Reduced Graphene Oxide

The scanning electron microscope (model JEOL JSM-7500F, Jeol, Tokyo, Japan) was used to study the coatings morphology with graphene oxide. The $(GO^+/GO^-)_n$ and $(GO^+/PSS)_n$ films formed on silicon wafers were investigated with the backscattered electron (BSE) detector. The samples were stuck on the cylinders and dried overnight before SEM imaging. The UV-Vis spectra measurements of the multilayer films with graphene oxide on quartz slides were conducted using Shimadzu Spectrophotometer UV-1800 (Shimadzu Corporation, Kyoto, Japan). The morphology of $(GO/GO)_n$ the films was imaged using Leica polarization microscope DM4000M equipped with an image analysis system, Sarfusoft 2.1 (Nanolane, Leica Microsystems GmbH, Wetzlar, Germany).

The four-point probe method of measuring material surface resistivity was used to study multilayer films with rGO. The measurements were conducted with a digital potentiostat ECI 1286 frequency response analyzer FRA 1250 (Solartron Analytical, Farnborough,

UK). This technique involves bringing four equally spaced probes in contact with a material of unknown resistance. The electric contacts at the sample surface with the same spacing were made by sputtering gold to achieve a thickness of 50 nm. The probe electrodes were made of the same material to minimize the thermoelectric effects. The current was passed through the outer probes and induced a voltage in the inner voltage probes, measured in the range of ±1 V. The input resistance of the reference electrode clamp was >10 [GΩ].

The resistance values obtained during the measurements were transformed to the appropriate surface resistance according to the following equation:

$$r = \frac{R \cdot a}{l} \quad (1)$$

where: R—measured film resistance [Ω], a—width of the substrate (1.5 cm for polyimide plate and 2 cm for quartz plate), and l—the distance between two electrodes to measure the voltage (0.67 cm). Each surface resistance result was the average obtained from three plates; each plate was measured fourfold. The error of the average was less than 10%, mostly due to the limited repeatability of the film formation procedure.

3. Results and Discussion

3.1. Characterization of Positively and Negatively Charged Graphene Oxide

The average size of negatively and positively charged GO was about 500 nm. The zeta potential of pristine GO^- was -45 ± 5 mV, whereas that of the modified GO^+ was $+45 \pm 5$ mV, respectively. Both values indicate good electrostatic stability (~6 months). The size distributions for GO^+ and GO^- (freshly prepared suspensions and after 6 months of storage) are illustrated in Figure S1 in the Supplementary Materials.

3.2. Characterization of $(GO^+/GO^-)_n$ and $(GO^+/PSS)_n$ Films

The $(GO^+/GO^-)_n$ and $(GO^+/PSS)_n$ coatings were built on three different surfaces: silicon wafers, quartz plates, and flexible polyimide foil (PI) using the LbL method. Figure 2 presents the relationship between the GO absorbance at 232 nm and the number of deposition cycles for films formed at the quartz plate. It shows the systematic and linear increase of the adsorbed amount of graphene oxide nanosheets. SEM images, presented in Figure 3, confirmed the continuous structure created by adsorbed GO nanosheets. Figure 4 shows the growth of surface coverage with the number of deposition cycles, illustrating the increased connectivity in the graphene nanosheets networks. The optical microscope images confirm the effective growth of films formed with (GO^+/GO^-).

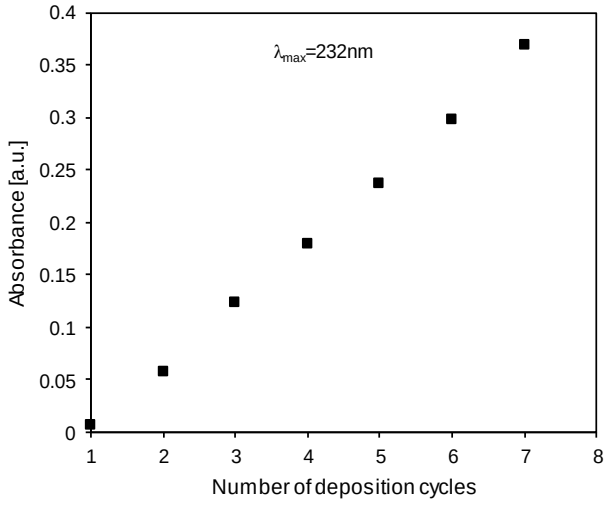

Figure 2. The dependence of the films' absorbance at λ_{max} = 232 nm on the number of (GO^+/GO^-) deposition cycles formed at quartz surfaces.

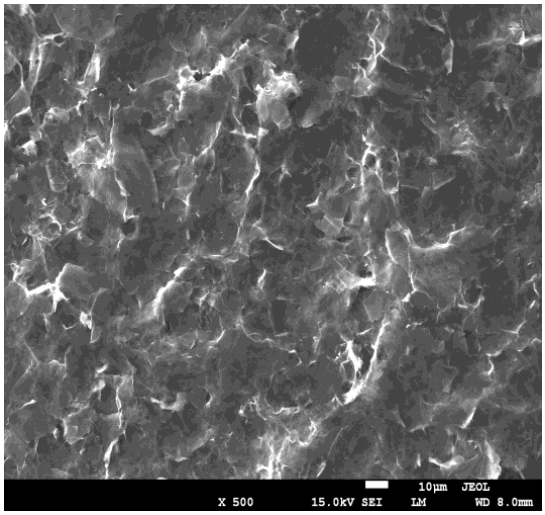

Figure 3. The example of SEM image of a film composed of GO^+ and GO^- deposited at silicon wafer. Image magnification 500×.

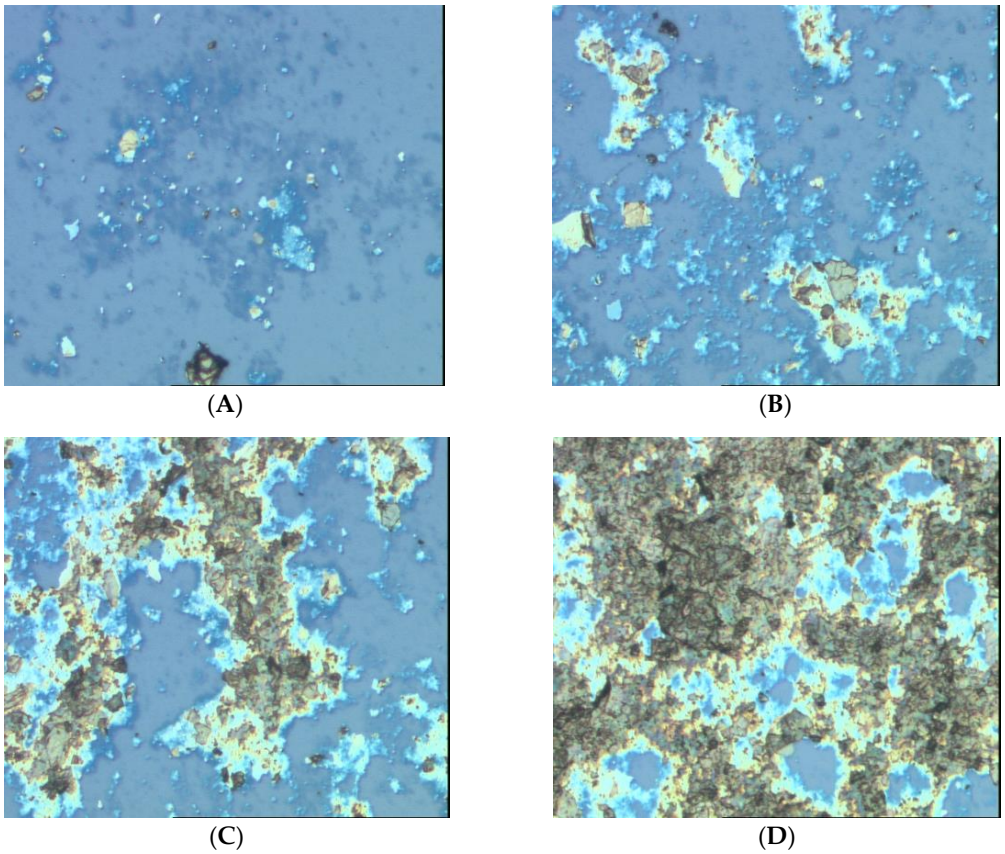

Figure 4. The Leica optical microscope DM4000M with Sarfusoft 2.1 system images showing the increase of surface coverage with the number of adsorbed deposition cycles $(GO^+/GO^-)_n$; (**A**) 1 deposition cycle, (**B**) 3, (**C**) 5, (**D**) 7 deposition cycles, respectively. Size of the image 100 μm × 100 μm.

3.3. Conductivity of Multilayer Films (rGO⁺/rGO⁻, rGO⁺/PSS)

The formation of the conductive multilayers by thermal reduction of GO was demonstrated by the decrease in the resistance of $(rGO^+/rGO^-)_n$ films. The surface conductivity of films was examined by measuring a sheet resistance (*R*s) of the film with a four-point probe. Figure 5 presents the sheet resistance of rGO containing multilayers as a function of the number of (rGO^+/rGO^-) cycles deposited on quartz (Figure 4A) and flexible polyimide

foil (PI) (Figure 4B) after thermal reduction of the deposited graphene oxide at various temperatures (150 °C, 180 °C and 250 °C). In all cases, the resistance decreased with the increasing reduction temperature and the values obtained at the reduction temperature of 180 °C and 250 °C on both substrates (quartz and polyimide foils) were significantly lower than at 150 °C.

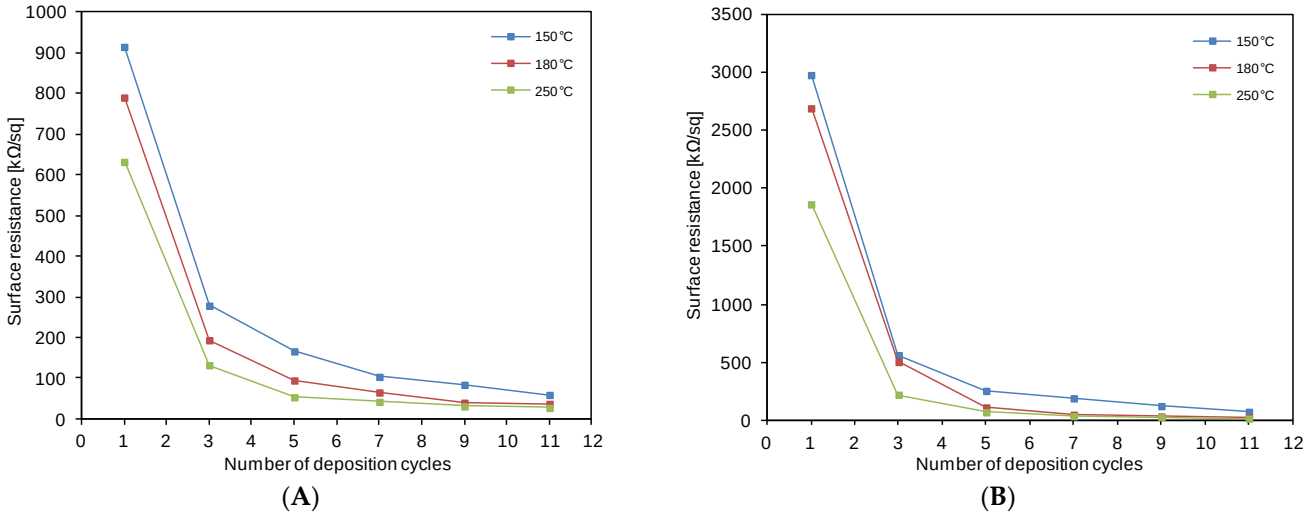

Figure 5. The dependence of surface resistance of multilayer films $(rGO^{+}/rGO^{-})_n$ on the number of deposition cycles; (**A**) on quartz plates, (**B**) on polyimide foil after thermal reduction at different temperatures (150 °C, 180 °C, 250 °C).

The sheet resistance (Figure 5) for the PEM's built at quartz support decreased from ~600–900 kΩ/sq to ~25–60 kΩ/sq (Figure 5A) with an increasing number of deposition cycles. The most substantial drop in the resistance was observed for films obtained by up to five deposition cycles; it decreased much more gradually for thicker ones. The high resistance of coatings for 1–3 bilayers can be attributed to the low number of interconnections in the network formed by plates of rGO (see Figure 4). Therefore, to reach the percolation threshold assuring good conductivity, at least five cycles need to be applied. Similar results were obtained for films on polyimide plates. Film resistance decreased from ~2000–3000 kΩ/sq to ~15–70 kΩ/sq with the number of deposition cycles (from 1 to 11, cf. Figure 5B). Although the reported specific resistance of quartz, 7.5×10^{17} Ω·m [51], is higher than polyimide, 1.3×10^{16} Ω·m [52], the larger resistance for the latter with the thin rGO films can be attributed to the conditions of their formation. The quartz plates are more homogeneous than polyimide foil, thus the resulting coatings are more uniform. The method of cleaning the substrates can also influence the formation of multilayers and sheet resistance measurements. The quartz plates' surface was cleaned and activated using "piranha solution," while the polyimide foil was cleaned using isopropanol. After the deposition of five cycles, the resistance becomes comparable, indicating that the film structure becomes independent of the type of support.

To better illustrate the improvement of the multilayers' conductive properties with the reduction temperature, we collected, in Tables 1 and 2, the lowest resistance values obtained for films adsorbed on the quartz and polyimide surfaces after 7, 9, and 11 deposition cycles. According to our previous results [32,33], the thermal method of the reduction of GO containing films at temperatures of 180 °C and higher leads to the formation of sp^2-bonded C atoms, and the decrease in the film resistance may be ascribed to the restoration of conjugated C=C bonds in the structure of rGO films.

Table 1. Summary of the results of the surface resistance values for films $(rGO^+/rGO^-)_n$ depending on the number of deposition cycles and the reduction temperature on quartz plates.

Film	Surface Resistance [kΩ/sq] Reduction Temp. 150 °C	Surface Resistance [kΩ/sq] Reduction Temp. 180 °C	Surface Resistance [kΩ/sq] Reduction Temp. 250 °C
$(rGO^+/rGO^-)_7$	104	65	42
$(rGO^+/rGO^-)_9$	84	40	31
$(rGO^+/rGO^-)_{11}$	59	37	27

Table 2. Summary of the results of the surface resistance values for films $(rGO^+/rGO^-)_n$ depending on the number of deposition cycles and the reduction temperature on polyimide plates.

Film	Surface Resistance [kΩ/sq] Reduction Temp. 150 °C	Surface Resistance [kΩ/sq] Reduction Temp. 180 °C	Surface Resistance [kΩ/sq] Reduction Temp. 250 °C
$(rGO^+/rGO^-)_7$	190	49	37
$(rGO^+/rGO^-)_9$	123	34	27
$(rGO^+/rGO^-)_{11}$	74	22	15

To compare the film resistance of purely rGO films with ones either containing rGO^- and polycation (PEI) [33] or rGO^+ and polyanion, we prepared films with positively charged graphene oxide and poly(sodium 4-styrenesulfonate) $(rGO^+/PSS)_n$, with different numbers of deposition cycles on quartz plates and polyimide foil. The results of the surface resistance measurements are shown in Figure 6. The tendency of the decrease in surface resistance with the number of deposited cycles was similar as for the films $(rGO^+/rGO^-)_n$. For the first deposited layers (at both substrates: quartz plate and polyimide foil), the resistance values are very high, while for the number of bilayers >3, we observe a substantial decrease in sheet resistance, i.e., an increase in conductivity. When we compare films composed of only graphene oxide $(rGO^+/rGO^-)_n$, we observe an approximately 25–30% decrease in resistance respectively to $(PEI/rGO^-)_n$ films [49]. Films made of $(rGO^+/PSS)_n$ present much weaker conductivity, about 50–60% lower compared to the previously studied $(PEI/rGO^-)_n$ films [33]. Thus, the use of modified graphene oxide with a positive surface charge in combination with polyanion $(rGO^+/PSS)_n$ for the construction of the film significantly worsened the conductive properties of the film compared to $(rGO^+/rGO^-)_n$ and $(PEI/GO^-)_n$ [33].

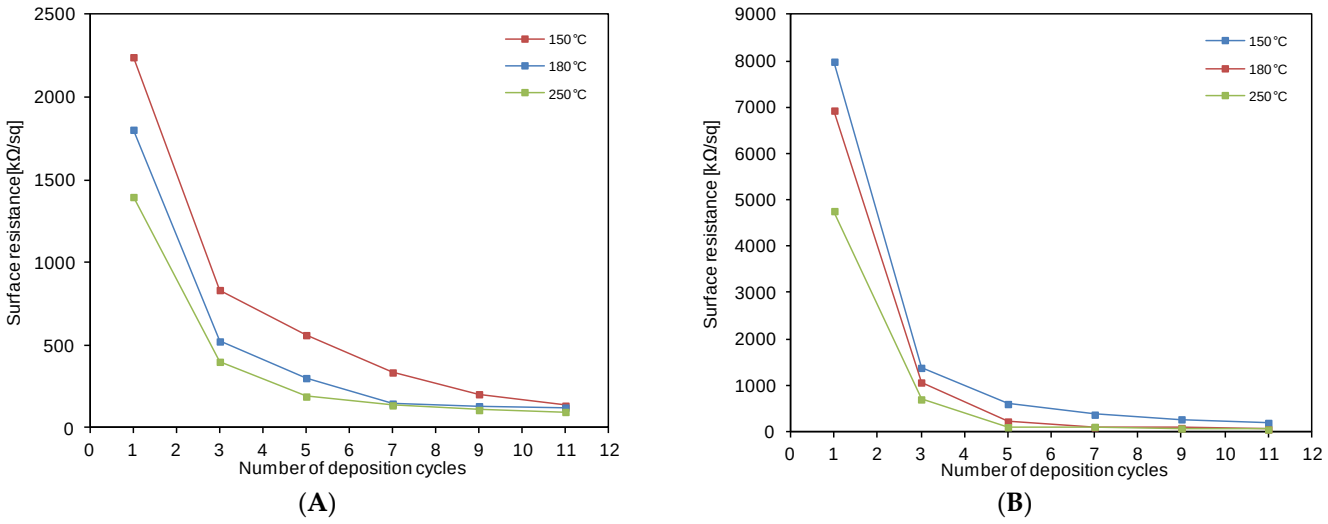

Figure 6. The dependence of surface resistance of multilayer films $(rGO^+/PSS)_n$ on the number of deposition cycles; (**A**) on quartz plates; (**B**) on polyimide foil after thermal reduction at different temperatures (150 °C, 180 °C, 250 °C).

Figure 7 illustrates the comparison of the sheet resistance of films formed by 11 deposition cycles film changes depending on the reduction temperature and film composition: $(PEI/rGO^-)_{11}$, $(rGO^+/rGO^-)_{11}$, and $(rGO^+/PSS)_{11}$. The sheet resistance values were presented for quartz substrate and the polyimide foil. They confirmed that for all reduction temperatures, the lowest surface resistance values were obtained for coatings made of $(rGO^+/rGO^-)_n$ compared to the other films. On the other hand, the $(rGO^+/PSS)_n$ films showed the highest values of the resistance out of the studied multilayers [33].

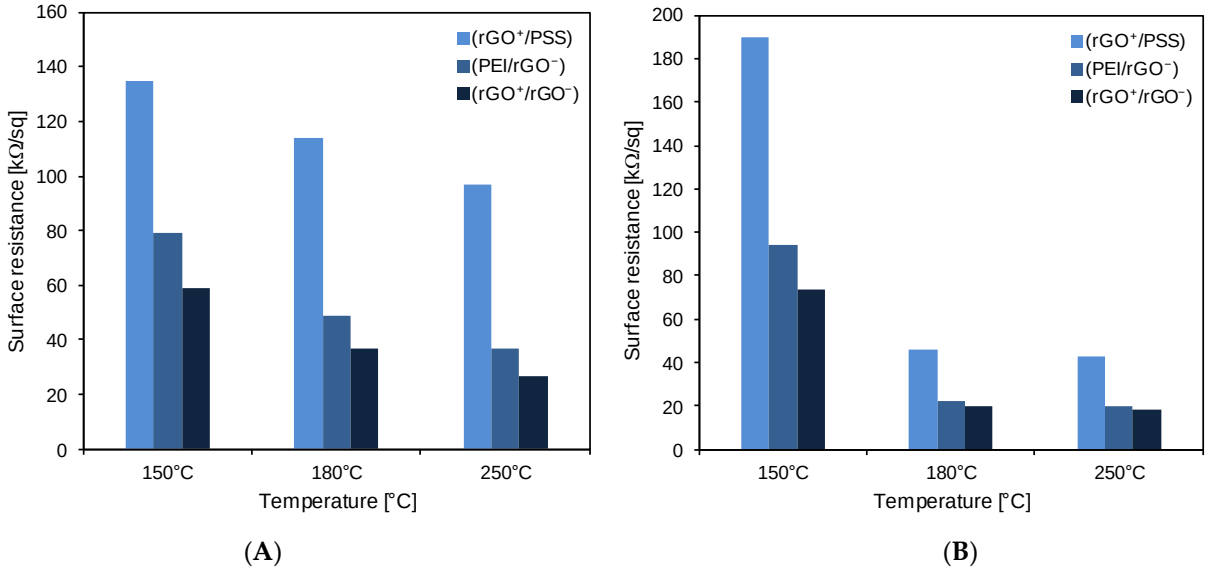

Figure 7. Dependence of the surface resistance values on the reduction temperature for (rGO^+/PSS), (PEI/rGO^-), (rGO^+/rGO^-) films formed by 11 deposition cycles on quartz plate (**A**) and polyimide foils (**B**).

In Table 3, the surface resistance values were compared for the multilayer films deposited on quartz plates, containing the comparable number of rGO layers, i.e., $(rGO^+/rGO^-)_5$, $(PEI/rGO^-)_{11}$, and $(rGO^+/PSS)_{11}$. We can conclude that the decrease in film resistance per one rGO layer is higher when rGO^- is combined in the multilayer with the polycation than with rGO^+. PEI is a non-conductive polymer, but most probably, its flexibility allows more optimal packing of graphene flakes for higher conductivity. Moreover, there are reports on decreasing graphene work function by PEI [53]. On the other hand $(rGO^+/PSS)_{11}$ was characterized by the highest resistance that can be caused by the lower conductivity of rGO^+ than rGO^-.

Table 3. The comparison of the surface resistance values for the multilayer films deposited on quartz plates, containing the comparable number of the rGO layers, i.e., $(rGO^+/rGO^-)_5$, $(PEI/rGO^-)_{11}$, and $(rGO^+/PSS)_{11}$.

Film	Surface Resistance [kΩ/sq] Reduction Temp. 150 °C	Surface Resistance [kΩ/sq] Reduction Temp. 180 °C	Surface Resistance [kΩ/sq] Reduction Temp. 250 °C
$(rGO^+/rGO^-)_5$	166	94	54
$(PEI/rGO^-)_{11}$	79	49	37
$(rGO^+/PSS)_{11}$	190	123	100

4. Conclusions

We presented a simple strategy for creating multilayer films of conducting reduced graphene oxide (rGO^+/rGO^-) by the LbL method. Films were constructed by the sequential deposition of negatively charged, pristine and chemically modified positively charged graphene oxide. We showed that the reduction at the temperature in the range of 180–250 °C provides high conductivity of the films due to the restoration of sp^2 carbon bonds in the graphene structure. The support surfaces exhibited a significant increase in

electric conductivity after depositing at least five $(rGO^+/rGO^-)_n$ cycles when the percolation threshold between rGO sheets was achieved. For films built by eleven deposition cycles, the sheet resistance of ~25 kΩ/sq in the case of ones formed on quartz plates, and ~15 kΩ/sq on polyimide plates, were reached. Concerning the film conductivity, the $(rGO^+/rGO^-)_n$ coatings appeared to be superior to films with the same number of deposited layers if either rGO^+ or rGO^- was accompanied by the oppositely charged polyelectrolyte. Such films can be an alternative to a high-cost graphene coatings. Our results may also suggest that the layer of rGO^+ obtained by the thermal reduction of graphene oxide modified by amidation can have lower conductivity than rGO^- received from the pristine GO. The application of $(rGO^+/rGO^-)_n$ films formed on polyimide foil allows for creating flexible, conductive material for new, advanced materials as low-cost, biocompatible, disposable sensors or biosensors.

Supplementary Materials: The following are available online at https://www.mdpi.com/article/10.3390/colloids5020020/s1, Figure S1: Size distribution measured by DLS for suspensions of GO^+ (A) and GO^- (B), freshly prepared and after 6 months of storage.

Author Contributions: Conceptualization, P.W.; methodology, T.K.; formal analysis, T.K. and P.W.; investigation, T.K.; writing—original draft preparation, T.K.; writing—review and editing, P.W.; visualization, T.K.; supervision, P.W. Both authors have read and agreed to the published version of the manuscript.

Funding: This work was partially funded by the statutory research funding of Jerzy Haber Institute of Catalysis and Surface Chemistry.

Data Availability Statement: The data presented in this study are available in text and supplementary materials.

Acknowledgments: The authors are grateful to Paweł Nowak for his invaluable help in surface resistivity measurements and Lilianna Szyk-Warszyńska for optical microscopy images.

Conflicts of Interest: The authors declare no conflict of interest.

References

1. Novoselov, K.S.; Geim, A.K.; Morozov, S.V.; Jiang, D.; Zhang, Y.; Dubonos, S.V.; Grigorieva, I.V.; Firsov, A.A. Electric field in atomically thin carbon films. *Science* **2004**, *306*, 666–669. [CrossRef] [PubMed]
2. Novoselov, K.S.; Jiang, D.; Schedin, F.; Booth, T.J.; Khotkevich, V.V.; Morozov, S.V.; Geim, A.K. Two-dimensional atomic crystals. *Proc. Natl. Acad. Sci. USA* **2005**, *102*, 10451–10453. [CrossRef] [PubMed]
3. Geim, A.K.; Novoselov, K.S. The rise of graphene. *Nat. Mater.* **2007**, *6*, 183–191. [CrossRef] [PubMed]
4. Bai, H.; Li, C.; Shi, G. Functional composite materials based on chemically converted graphene. *Adv. Mater.* **2011**, *23*, 1089–1115. [CrossRef]
5. Peressi, M. Surface Functionalization of Graphene. In *Graphene Chemistry: Theoretical Perspectives*; John Wiley & Sons, Ltd.: Chichester, UK, 2013; pp. 233–253. ISBN 9781118691281.
6. Vieira, N.C.S.; Borme, J.; MacHado, G.; Cerqueira, F.; Freitas, P.P.; Zucolotto, V.; Peres, N.M.R.; Alpuim, P. Graphene field-effect transistor array with integrated electrolytic gates scaled to 200 mm. *J. Phys. Condens. Matter* **2016**, *28*, 085302. [CrossRef] [PubMed]
7. Dreyer, D.R.; Park, S.; Bielawski, C.W.; Ruoff, R.S. The chemistry of graphene oxide. *Chem. Soc. Rev.* **2010**, *39*, 228–240. [CrossRef] [PubMed]
8. Li, D.; Müller, M.B.; Gilje, S.; Kaner, R.B.; Wallace, G.G. Processable aqueous dispersions of graphene nanosheets. *Nat. Nanotechnol.* **2008**, *3*, 101–105. [CrossRef]
9. Li, C.; Adamcik, J.; Mezzenga, R. Biodegradable nanocomposites of amyloid fibrils and graphene with shape-memory and enzyme-sensing properties. *Nat. Nanotechnol.* **2012**, *7*, 421–427. [CrossRef]
10. Pei, S.; Cheng, H.M. The reduction of graphene oxide. *Carbon N. Y.* **2012**, *50*, 3210–3228. [CrossRef]
11. Mao, S.; Pu, H.; Chen, J. Graphene oxide and its reduction: Modeling and experimental progress. *RSC Adv.* **2012**, *2*, 2643–2662. [CrossRef]
12. Moon, I.K.; Lee, J.; Ruoff, R.S.; Lee, H. Reduced graphene oxide by chemical graphitization. *Nat. Commun.* **2010**, *1*, 1–6. [CrossRef] [PubMed]
13. Fan, Z.; Wang, K.; Wei, T.; Yan, J.; Song, L.; Shao, B. An environmentally friendly and efficient route for the reduction of graphene oxide by aluminum powder. *Carbon N. Y.* **2010**, *48*, 1686–1689. [CrossRef]
14. Kuila, T.; Mishra, A.K.; Khanra, P.; Kim, N.H.; Lee, J.H. Recent advances in the efficient reduction of graphene oxide and its application as energy storage electrode materials. *Nanoscale* **2013**, *5*, 52–71. [CrossRef]

15. Paredes, J.I.; Villar-Rodil, S.; Martínez-Alonso, A.; Tascón, J.M.D. Graphene oxide dispersions in organic solvents. *Langmuir* **2008**, *24*, 10560–10564. [CrossRef] [PubMed]
16. Kim, J.; Cote, L.J.; Kim, F.; Yuan, W.; Shull, K.R.; Huang, J. Graphene oxide sheets at interfaces. *J. Am. Chem. Soc.* **2010**, *132*, 8180–8186. [CrossRef] [PubMed]
17. Kuziel, A.W.; Milowska, K.Z.; Chau, P.L.; Boncel, S.; Koziol, K.K.; Yahya, N.; Payne, M.C. The True Amphipathic Nature of Graphene Flakes: A Versatile 2D Stabilizer. *Adv. Mater.* **2020**, *32*, 2000608. [CrossRef]
18. Yu, W.; Sisi, L.; Haiyan, Y.; Jie, L. Progress in the functional modification of graphene/graphene oxide: A review. *RSC Adv.* **2020**, *10*, 15328–15345. [CrossRef]
19. Faghani, A.; Donskyi, I.S.; Fardin Gholami, M.; Ziem, B.; Lippitz, A.; Unger, W.E.S.; Böttcher, C.; Rabe, J.P.; Haag, R.; Adeli, M. Controlled Covalent Functionalization of Thermally Reduced Graphene Oxide To Generate Defined Bifunctional 2D Nanomaterials. *Angew. Chem. Int. Ed.* **2017**, *56*, 2675–2679. [CrossRef] [PubMed]
20. Güneş, F.; Shin, H.J.; Biswas, C.; Han, G.H.; Kim, E.S.; Chae, S.J.; Choi, J.Y.; Lee, Y.H. Layer-by-layer doping of few-layer graphene film. *ACS Nano* **2010**, *4*, 4595–4600. [CrossRef]
21. Kim, M.S.; Kim, M.; Son, S.; Cho, S.Y.; Lee, S.; Won, D.K.; Ryu, J.; Bae, I.; Kim, H.M.; Kim, K.B. Sheet Resistance Analysis of Interface-Engineered Multilayer Graphene: Mobility Versus Sheet Carrier Concentration. *ACS Appl. Mater. Interfaces* **2020**, *12*, 30932–30940. [CrossRef] [PubMed]
22. Xu, Y.; Bai, H.; Lu, G.; Li, C.; Shi, G. Flexible graphene films via the filtration of water-soluble noncovalent functionalized graphene sheets. *J. Am. Chem. Soc.* **2008**, *130*, 5856–5857. [CrossRef] [PubMed]
23. Kong, B.S.; Geng, J.; Jung, H.T. Layer-by-layer assembly of graphene and gold nanoparticles by vacuum filtration and spontaneous reduction of gold ions. *Chem. Commun.* **2009**, 2174–2176. [CrossRef]
24. Hong, W.; Xu, Y.; Lu, G.; Li, C.; Shi, G. Transparent graphene/PEDOT-PSS composite films as counter electrodes of dye-sensitized solar cells. *Electrochem. Commun.* **2008**, *10*, 1555–1558. [CrossRef]
25. Cote, L.J.; Kim, F.; Huang, J. Langmuir-blodgett assembly of graphite oxide single layers. *J. Am. Chem. Soc.* **2009**, *131*, 1043–1049. [CrossRef] [PubMed]
26. Milošević, I.R.; Vasić, B.; Matković, A.; Vujin, J.; Aškrabić, S.; Kratzer, M.; Griesser, T.; Teichert, C.; Gajić, R. Single-step fabrication and work function engineering of Langmuir-Blodgett assembled few-layer graphene films with Li and Au salts. *Sci. Rep.* **2020**, *10*, 1–12. [CrossRef]
27. Decher, G.; Hong, J.-D. Buildup of ultrathin multilayer films by a self-assembly process, 1 consecutive adsorption of anionic and cationic bipolar amphiphiles on charged surfaces. *Makromol. Chem. Macromol. Symp.* **1991**, *46*, 321–327. [CrossRef]
28. Cassagneau, T.; Guérin, F.; Fendler, J.H. Preparation and characterization of ultrathin films layer-by-layer self-assembled from graphite oxide nanoplatelets and polymers. *Langmuir* **2000**, *16*, 7318–7324. [CrossRef]
29. Shen, J.; Hu, Y.; Li, C.; Qin, C.; Shi, M.; Ye, M. Layer-by-layer self-assembly of graphene nanoplatelets. *Langmuir* **2009**, *25*, 6122–6128. [CrossRef] [PubMed]
30. Lee, D.W.; Hong, T.K.; Kang, D.; Lee, J.; Heo, M.; Kim, J.Y.; Kim, B.S.; Shin, H.S. Highly controllable transparent and conducting thin films using layer-by-layer assembly of oppositely charged reduced graphene oxides. *J. Mater. Chem.* **2011**, *21*, 3438–3442. [CrossRef]
31. Yang, M.; Hou, Y.; Kotov, N.A. Graphene-based multilayers: Critical evaluation of materials assembly techniques. *Nano Today* **2012**, *7*, 430–447. [CrossRef]
32. Pajor-Świerzy, A.; Kruk, T.; Warszyński, P. Enhancement of the Electrocatalytic Properties of Prussian Blue Containing Multilayer Films Formed by Reduced Graphene Oxide. *Colloids Interface Sci. Commun.* **2014**, *1*, 6–9. [CrossRef]
33. Kruk, T.; Socha, R.P.; Szyk-Warszyńska, L.; Warszyński, P. Flexible and ultrathin polyelectrolyte conductive coatings formed with reduced graphene oxide as a base for advanced new materials. *Appl. Surf. Sci.* **2019**, *484*, 501–510. [CrossRef]
34. Kotov, N.A.; Dékány, I.; Fendler, J.H. Ultrathin graphite oxide-polyelectrolyte composites prepared by self-assembly: Transition between conductive and non-conductive states. *Adv. Mater.* **1996**, *8*, 637–641. [CrossRef]
35. Kovtyukhova, N.I. Layer-by-layer assembly of ultrathin composite films from micron-sized graphite oxide sheets and polycations. *Chem. Mater.* **1999**, *11*, 771–778. [CrossRef]
36. Yang, Y.-H.; Bolling, L.; Priolo, M.A.; Grunlan, J.C. Graphene: Super Gas Barrier and Selectivity of Graphene Oxide-Polymer Multilayer Thin Films (Adv. Mater. 4/2013). *Adv. Mater.* **2013**, *25*, 493. [CrossRef]
37. Chen, J.T.; Fu, Y.J.; An, Q.F.; Lo, S.C.; Huang, S.H.; Hung, W.S.; Hu, C.C.; Lee, K.R.; Lai, J.Y. Tuning nanostructure of graphene oxide/polyelectrolyte LbL assemblies by controlling pH of GO suspension to fabricate transparent and super gas barrier films. *Nanoscale* **2013**, *5*, 9081–9088. [CrossRef] [PubMed]
38. Zhao, L.; Zhang, H.; Kim, N.H.; Hui, D.; Lee, J.H.; Li, Q.; Sun, H.; Li, P. Preparation of graphene oxide/polyethyleneimine layer-by-layer assembled film for enhanced hydrogen barrier property. *Compos. Part B Eng.* **2016**, *92*, 252–258. [CrossRef]
39. Gross, M.A.; Sales, M.J.A.; Soler, M.A.G.; Pereira-Da-Silva, M.A.; Da Silva, M.F.P.; Paterno, L.G. Reduced graphene oxide multilayers for gas and liquid phases chemical sensing. *RSC Adv.* **2014**, *4*, 17917–17924. [CrossRef]
40. do Santos, F.A.; Vieira, N.C.S.; Zambianco, N.A.; Janegitz, B.C.; Zucolotto, V. The layer-by-layer assembly of reduced graphene oxide films and their application as solution-gated field-effect transistors. *Appl. Surf. Sci.* **2021**, *543*, 148698. [CrossRef]
41. Lee, T.; Min, S.H.; Gu, M.; Jung, Y.K.; Lee, W.; Lee, J.U.; Seong, D.G.; Kim, B.S. Layer-by-Layer Assembly for Graphene-Based Multilayer Nanocomposites: Synthesis and Applications. *Chem. Mater.* **2015**, *27*, 3785–3796. [CrossRef]

42. Kim, S.M.; Joo, P.; Ahn, G.; Cho, I.H.; Kim, D.H.; Song, W.K.; Kim, B.S.; Yoon, M.H. Transparent conducting films based on reduced graphene oxide multilayers for biocompatible neuronal interfaces. *J. Biomed. Nanotechnol.* **2013**, *9*, 403–408. [CrossRef] [PubMed]
43. Jijie, R.; Kahlouche, K.; Barras, A.; Yamakawa, N.; Bouckaert, J.; Gharbi, T.; Szunerits, S.; Boukherroub, R. Reduced graphene oxide/polyethylenimine based immunosensor for the selective and sensitive electrochemical detection of uropathogenic Escherichia coli. *Sens. Actuators B Chem.* **2018**, *260*, 255–263. [CrossRef]
44. Zhu, J.; He, J. Assembly and benign step-by-step post-treatment of oppositely charged reduced graphene oxides for transparent conductive thin films with multiple applications. *Nanoscale* **2012**, *4*, 3558–3566. [CrossRef]
45. Eda, G.; Fanchini, G.; Chhowalla, M. Large-area ultrathin films of reduced graphene oxide as a transparent and flexible electronic material. *Nat. Nanotechnol.* **2008**, *3*, 270–274. [CrossRef]
46. Becerril, H.A.; Mao, J.; Liu, Z.; Stoltenberg, R.M.; Bao, Z.; Chen, Y. Evaluation of solution-processed reduced graphene oxide films as transparent conductors. *ACS Nano* **2008**, *2*, 463–470. [CrossRef] [PubMed]
47. Wang, X.; Zhi, L.; Tsao, N.; Tomović, Ž.; Li, J.; Müllen, K. Transparent carbon films as electrodes in organic solar cells. *Angew. Chem. Int. Ed.* **2008**, *47*, 2990–2992. [CrossRef]
48. Yamaguchi, H.; Eda, G.; Mattevi, C.; Kim, H.K.; Chhowalla, M. Highly uniform 300 mm wafer-scale deposition of single and multilayered chemically derived graphene thin films. *ACS Nano* **2010**, *4*, 524–528. [CrossRef]
49. Park, J.S.; Cho, S.M.; Kim, W.J.; Park, J.; Yoo, P.J. Fabrication of graphene thin films based on layer-by-layer self-assembly of functionalized graphene nanosheets. *ACS Appl. Mater. Interfaces* **2011**, *3*, 360–368. [CrossRef]
50. Hwang, H.; Joo, P.; Kang, M.S.; Ahn, G.; Han, J.T.; Kim, B.S.; Cho, J.H. Highly tunable charge transport in layer-by-layer assembled graphene transistors. *ACS Nano* **2012**, *6*, 2432–2440. [CrossRef]
51. Helmenstine, A.M.P. Resistivity Table/Chart for Common Materials | Electronics Notes. Available online: https://www.electronics-notes.com/articles/basic_concepts/resistance/electrical-resistivity-table-materials.php (accessed on 9 March 2021).
52. Overview of Materials for Polyimide. Available online: http://www.matweb.com/search/DataSheet.aspx?MatGUID=ab35b368ab9c40848f545c35bdf1a672&ckck=1 (accessed on 9 March 2021).
53. Cha, M.J.; Song, W.; Kim, Y.; Jung, D.S.; Jung, M.W.; Lee, S.I.; Adhikari, P.D.; An, K.S.; Park, C.Y. Long-term air-stable n-type doped graphene by multiple lamination with polyethyleneimine. *RSC Adv.* **2014**, *4*, 37849–37853. [CrossRef]